SRD ENGINEERING INCORPORATED

A SHEAR MOMENT MODEL

FOR

PRESTRESSED CONCRETE BEAMS

by
PAUL F. CSAGOLY

Prepared for the FLORIDA DEPARTMENT OF TRANSPORTATION State
Project No. 9900-1550
WDI No. 0110209
Contract No. C-3879
ID No. VS592222789

December, 1991

CONTENT

1 INTRODUCTION

In excess of 1,300 AASHTO IV beams were prefabricated for the approaches of the Florida Sunshine Skyway Bridge over the Tampa Bay entrance. The endzones of some of these prestressed concrete beams showed honey-combing and cracking, indicating the possibility of reduced shear resistance. Pilot tests which were carried out on two such beams had confirmed this possibility. Subsequently, under the aegis of the Florida Department of Transportation, this author performed 16 shear tests on eight AASHTO IV beams, specially fabricated, in order to determine the cause(s) of the substandard performance observed. There were three independent variables involved, namely:

a/ 50% shielding or no shielding of the strands,

b/ confinement or no confinement cage in the end zone, and

c/ coated or uncoated web steel.

It was found that on the average the unshielded beams possessed 19.9% more shear resistance than the: shielded ones, the beams with confinement steel - 13.2% more than those without, and beams with uncoated web steel - 6.9% more than those with coated bars. The strongest beam, being favored by all the three variables, had a shear resistance of 393.1 KIPS, being 45.1% above the weakest beam which broke at 271.0 KIPS. The latter reflects the Florida design standards of 1985 which had immediately been changed, in response to the test results, by limiting the number of shielded strands to 25%, and mandating the application of confinement reinforcement. The expected increase in shear resistance due to these two changes was:

$$100 \times ((1 + 0.5x0{:}199)(1 + 0.132) - 1) = 24.5\%$$

It is of interest to note that neither the ACI-AASHTO nor any other known design formula currently incorporates the effects of these three variables in the shear design of prestressed concrete beams.

The shear span for all the 16 tests was 75 inches, or about 1.21 times the structural height of the specimen, including the 54 inches tall beam and the 8 inches deep concrete slab.

Regardless of the combination of variables, the failure pattern was observed to be remarkably identical. In all cases, several diagonal web cracks developed, one of which - not necessarily the first or last that had appeared - dilated out-of proportion to the others. This crack, which will be referred herein to as the SIGNIFICANT CRACK or "S" crack, had completely separated the bottom chord, the web, and had been confined to the bottom part of the top chord (the slab) by what appeared to be a compression zone. This crack was invariably large enough to preclude the existance of aggregate interlock, and formed a nearly trapezoidal segment wanting to separate from the main body of the beam. The "S" crack invariably intercepted the development length, even at times the transfer length. The failure was always precipitated by the slip of strands, after which a considerable resistance had been retained,, but the peak value had never been regained.

The apparent uniformity of the mode of failures indicated the probable presence of a mechanical shear-moment model, which is first introduced in this report, and will be referred to as the "CS" shear model.

Since 1985 a considerable number of valid shear tests have been carried out in the United States and Canada, of which the following are known to this author:

Dr. Shahawy - Florida DOT

Drs. Kaufman & Ramirez - Purdue University

Drs. Maruyama & Rizkalla - University of Manitoba, and

Drs. Deatherage & Burdette - University of Tennessee.

With the exception of one Purdue test in which failure was caused by web crushing, all the tests reviewed for this report - either in-depth or superficially- indicated the presence of the same mechanical model, even if the failure mode was essentially flexural.

The intact appearance of the compression zone was also observed by others. Reference 1 suggests that "After slippage, all beams exhibited large crack widths and excessive deformation before failure. This behavior suggested that failure of beams is mainly controlled by the condition of concrete in the compression zone." and "The concrete in the compression zone was neither punched nor crushed."

Reference 1 also brings attention to the import of the "S" crack intercepting the strands within the development length. "However, the current code recommendation for the development length for pre-tensioned strands should be modified to include the shear crack effect, or the length should be measured from the point where the shear crack crosses the strands."

2 THE "CS" SHEAR MODEL

As illustrated in Figure 1, the "CS" shear model is defined by the geometry of the breakaway segment, and by the internal and external forces acting thereon. Geometry:

line A-B: top of beam, or top of concrete slab in case of composite action,

line B-C: plastic compression zone, height "c",

line C-D: location of significant crack,

line D-E: crack of no import below the center of gravity of active strands,

line E-F: bottom of beam, and

line F-A: end of beam.

and:

g: bonded length of prestressing strands,

d: distance between the center of gravity of shear steel in yield and line B-C,

q: internal moment arm of lateral forces.

The model is based on equilibria of external and internal forces for both moment and shear:

Outer moment M_o due to reaction force R, weight of segment W and any superimposed load P.

Outer shear V_o due to same as above.

Internal moment $H_{st}q$, where H_{st} is either the bonded resistance or the ultimate tensile resistance of the active strands, whichever is smaller, plus $V_s d$ due to the web steel at yield.

In the absence of any outside horizontal force: $H_{st} = N_c$, therefore:

$M_o = H_{st}q + V_s d$ and

$V_o = V_s + V_c$

3 RELATIONSHIP BETWEEN V_c AND N_c

Figure 2 depicts the distributions assumed for compressive and shear stresses within the compression zone. If the area of the compression zone is A_c, then:

$N_c = f_x A_c$ and $V_c = 2v_c A_c/3$

When stresses f_x and v_c are combined at the bottom of the compression zone, a pair of principal stresses result, one compressive and one tensile. It is obvious that at ultimate limit state the compressive principal stress f_2 cannot exceed the crushing strength of concrete f'_c, and that the tensile principal stress f_1 cannot exceed the tensile strength of the concrete, defined as $k\sqrt{f'_c}$. For determining the principal stresses in question the Mohr circle can be used, for being valid in both elastic and inelastic phases.

From textbook: $\tan 2\theta = 2v_c f_x$ where θ is the angle between f_2 and f_x as shown in Figure 3. From the theory of principal stresses:

$f_1 = \frac{1}{2}(f_x - f_x(1 + 4v_c^2/f_x^2)^{\frac{1}{2}}) = 0.5f_x(1 - (1 + \tan^2 2\theta)^{\frac{1}{2}}) =$

$= - f_x \sin^2\theta / (\cos^2\theta - \sin^2\theta) = - k(f_c')^{\frac{1}{2}}$, then

$(\cos^2\theta - \sin^2\theta)/\sin^2\theta = f_x/k(f_c')^{\frac{1}{2}} = N_c/A_c k(f_c')^{\frac{1}{2}} = n_1$

from which: $\text{cotan}^2\theta = n_1 + 1$

Similarly:

$f_2 = \frac{1}{2}(f_x + f_x(1 + 4v_c^2/f_x^2)^{\frac{1}{2}}) = 0.5f_x(1 + (1 + \tan^2 2\theta)^{\frac{1}{2}}) =$

$= + f_x \cos^2\theta / (\cos^2\theta - \sin^2\theta) = f_c'$, then

$(\cos^2\theta - \sin^2\theta)/\cos^2\theta = f_x/f_c' = N_c/A_c f_c' = n_2$

from which: $\text{cotan}^2\theta = 1/(1 - n_2)$

When both limit states are simultaneously satisfied:

$n_1 + 1 = 1/(1 - n_2)$

After substituting the appropriate expressions for n_1 and n_2, the following equation is obtained for the compressive area: $A_c = N_c/(f_c' - k(f_c')^{\frac{1}{2}})$

If $f_c'' = f_c' - k(f_c')^{\frac{1}{2}}$ then $A_c = N_c/f_c''$

After some further manipulation of the equations:

$V_c = 2N_c ((1 + k(f_c')^{\frac{1}{2}}/f_c'')k(f_c')^{\frac{1}{2}}/f_c'')^{\frac{1}{2}} /3$

This last expression for V_c is conveniently void of both the compressive area A_c and the angle θ. It is the product of three values, namely:

2/3 - the shape factor for the assumed parabolic distribution of shear stresses; if the assumed shape is found somewhat incorrect by future research, the factor can be easily corrected,

$((1 + k(f_c')^{\frac{1}{2}}/f_c'')k(f_c')^{\frac{1}{2}}/f_c'')_{\frac{1}{2}}$ - a sole function of concrete strength properties,

N_c - the compression force.

In other words, for a given concrete strength, the relationship between the shear and compressive forces in the concrete is simply $V_c = rN_c$, by which the shear component carried by the concrete can directly be calculated. The current AASHTO Bridge Specifications allow k = 6.0, and the new AASHTO Code is expected to permit k = 7.5. Both values are somewhat on the conservative side. A better approximation for tensile strength can be obtained from Reference 2, where a statistical analysis of 34 data points resulting from tensile tests at the 95% level yields k = 8.6. Table 1 provides f_c'' and r values for both k = 7.5 and k = 8.6 for all practically used concrete strengths at 500 PSI intervals. It can be seen that k = 8.6 offers an average increase of 9.25% over k = 7.5 in terms of shear resistance.

4 DISTRIBUTION OF BOND

Where the significant crack intercepts the development length of the prestressing strands, the bonded or anchored strength of the strands should be calculated on the basis of bond stress distribution between the crack and the end of the beam. Current codes provide only for the transfer and development lengths, therefore cannot directly be used in conjunction with the mechanical shear model. In the following, continuous bond stress distribution is determined by applying the data provided in Reference 3 and current ACI. As illustrated in Figure 4, Ref. 3 provides for the slope of the cumulative distribution curve at x = 0. Two data points are borrowed from ACI:

H_t - force at transfer, l_t - transfer length, and

H_u - force at ultimate, l_d - development length.

With the given pieces of information, a third-order parabolic curve can be established: $H = ax + bx^2 + cx^3$

for which: $dH/dx = a + 2bx + 3cx^2$ is the distribution of bond stresses.

at $x = 0$ $dH/dx = a = mH_t/l_t$

at $x = l_t$ $H_t = al_t + bl_t^2 + cl_t^3$

at $x = l_d$ $H_d = al_d + bl_d^2 + cl_d^3$

which yield:

$b = (H_t l_d^3 - H_d l_t^3 - mH_t l_d(l_d^2 - l_t^2))/l_t l_d(l_d - l_t)$ and

$c = (H_t l_d^2 - H_d l_t^2 - mH_t l_d(l_d - l_t))/l_t l_d(l_t - l_d)$

0.5" diameter strand, assumed values:

$A_{st} = 0.153$ in^2, $m = 1.43$

$H_t = 162.0 \times 0.153 = 24.79$ KIPS, and $l_t = 30$ in.

$H_d = 270.0 \times 0.153 = 41.31$ KIPS, and $l_d = 80$ in.

yield: $a = +1.1817$ KIP/in.

$b = -0.01396$ KIP/in^2

$c = +0.07056 \times 10^{-3}$ KIP/in^3

0.6" diameter strand, assumed values:

$A_{st} = 0.217$ in^2, $m = 1.43$

$H_t = 163.3 \times 0.217 = 35.44$ KIPS, and $l_t = 35$ in.

$H_d = 270.0 \times 0.217 = 58.59$ KIPS, and $l_d = 100$ in.

yield: $a = +1.4361$ KIP/in.

$b = -0.01450$ KIP/in^2

$c = +0.05876 \times 10^{-3}$ KIP/in^3

Table 2 contains calculated H_x values for both strands at 5.0 inch intervals. It can be seen that that the curves do not have discontinuity at $x = l_t$ - but unreported information is available to indicate that in reality a smooth curve is more appropriate than the theoretical one reflected by the ACI Code. It is obvious that further research is needed to refine or to correct these curves, which are based on skeletal information.

5 EQUILIBRIUM OF WEB FORCES

The scope of work for this report does not include the establishment of an appropriate method of searching for the angle β of the significant crack. Tests seem to indicate that the first diagonal crack, which reflects maximum tensile stresses in the elastic phase, only occasionally develops into being the significant crack. Both the location and the angle of the significant crack may be different from those of the first one, indicating a considerable re-arrangement of web forces in the inelastic phase. The following derivation may be applied to locate the significant crack.

Figure 6 illustrates the forces acting at a panel point, which is the intersection of a stirrup (or pair of) and the center line of active strands in the bottom chord. Acting at this point also is the diagonal compression force D. Normally the force ΔH_{st}, defined as the increase in the H_{st} force within the boundaries of vertical strip of s width, cannot be determined a priori, consequently neither the magnitude nor the inclination of D can directly be computed. But the distribution of cumulative bond stresses, as discussed in Chapter 4, permits determining ΔH_{st} with a degree of certainty.

$$\Delta V_s = f_y A_s$$

$$\Delta H_{st} = H_{x2} - H_{x1}$$

$$\tan\beta = V_s / H_{st}$$

$$D = \Delta V_s / \sin\beta$$

then the diagonal concrete compressive stress:

$f_{cd} = D/bs.\sin\beta = A_s f_y / bs.\sin^2\beta$, where b is the width of the web.

e.g

pair of #5 stirrups at 10.0 inch centers,

20 - 0.5" diameter strands with x_1 = 35 in. and x_2 = 45 in.

A_s = 2 x 0.31 = 0.62 in^2, and b = 6.0 in.

from Table 2: ΔH_{st} = 20(31.32 - 27.26) = 81.2 KIPS

ΔV_s = 0.62 x 60.0 = 37.2 KIPS

$\tan \beta$ = 37.2 / 81.2 = 0.4581 so β = 24.6°

f_{cd} = 3,574 PSI.

6 ROLE OF CONFINEMENT STEEL

Over the years several jurisdictions abandoned the confinement steel, as well as the end block, in order to reduce cost of pre-cast, pre-stressed concrete beams. This change was supported by several tests, either carried out or sponsored by PCA. The majority of these tests, both static and dynamic, included third-point loading, by which - as it is known now - the environment leading to serious inelastic straining of and subsequent shear failure in the end zone may not easily be attained, as the beam tends to fail in flexure.

In an appropriate shear test, the -shear span "a" should not normally exceed 2.0 t0 2.5 times the structural height "h" of the beam. The 1985 Florida DOT tests - with a = 1.20h - were therefore valid shear tests. They all exhibited pronounced longitudinal cracking at the level of strand rows, as well as at the center line of the bottom of the lower flange. As mentioned in the Introduction, the presence of confinement steel increased the shear resistance at the ultimate by an average of 13.2%.

Obviously the cracks observed at the level of strands must have been caused by the wedge - or Hoyer - effect of the strands. The following is a plausible explanation for the crack in the bottom. As exhibited in Figure 7, a strut-and-tie model can be drawn to approximate the magnitude of transverse splitting force T, resulting from the spreading of the reaction force R above the bearing.

For an AASHTO IV beam T = 0.161 R, which translates to 56.3 KIPS for a 350.0 KIP reaction force. This T force, depending on other factors such as the lateral bearing resistance, resistance by the horizontal stirrup legs and the , longitudinal distribution of the T force, may conceivably cause cracking. If the significant crack penetrates the end zone, where confinement steel is present, such steel is incorporated in the calculated force Vs. There is no way, however, at least none is known to this author, by which the enhancement of bond due to confinement may be assessed with confidence. Consequently only the direct shear effect of this steel is considered in this report.

7 FLOW CHART AND SAMPLE CALCULATIONS

The proposed shear model represents a major deviation from any approach currently codified for the- design of prestressed concrete beams. Major such deviations, in. no intended order of import, are:

a/ No shear is transmitted in the web concrete by aggregate interlock, or by any other structural action.

b/ Shear is transmitted by the compressive part of the flange.

c/ Shear transmitted by the concrete is a direct function of the concrete material and the compression force.

d/ The confinement steel is contributing to the web steel where applicable.

e/ The active strand force is determined from curves or charts derived from valid bond tests.

f/ Complete equilibrium exists between external and internal forces.

As shown on the flow-chart in Figure 8, the first step is to calculate the external shear V_o and moment M_o, determined from test results, at the center of compression zone line B-C, as shown in Figure 1. In a design case, the

extreme shear and the simultaneous moment are to be sought, since the moment tends to increase the shear resistance. Next the crack, as determined from the test, is drawn over the web steel elevation, as indicated in Figure 9, in order to establish the web steel that is acting through the significant crack. Smeared steel distribution A_s/s, as normally assumed in shear design, should not be used, since the intensity of steel may change - in some cases more than once - within the crack. If present, the effect of confinement steel should be considered. Steel, being too close to either end of the crack, may subjectively be discounted for the potential lack of adequate anchorage. Yield point f_y may be taken at nominal value, or at the tested value if such information is available. In calculating the moment of V_s about the B-C line, non-uniform distribution of web steel should be taken into account.

The moment $M_{st} = H_{st}.q$ is by definition the difference between the external moment M_o and the steel moment M_s. For combinations of low shear and high moment, the angle β is approaching 90°, and M_s zero, consequently the latter has only formative significance. Next, as usual, the internal moment arm "q" is determined in an iterative manner, yielding compression force N_c and $V_c = r.N_c$. If the sum $V_c + V_s$ is less than V_o, the mode of failure is shear. As derived in Chapter 4, the anchored strength H_{st} of the active strands can now be calculated. In case of shielded strands, the origin of the curve should be taken at the end of shielding. If H_{st} is less than N_c , the failure mode is slippage; if H_{st} exceeds the ultimate tensile resistance H_u of the strands, the failure mode is flexure.

In the following three worked examples are presented, two of which are on a Florida DOT test beam designated as A1-00-M, and the third is on a continuous, voided deck structure reported in Reference 4.

A1-00-M

As illustrated in Figure 9, this specimen consisted of an AASHTO II beam composite with a slab of 42 in. width and 8 in. depth. It had 16 - 0.5" diameter strands, unshielded (indicated by -00-), #3 bars as confinement steel, and minimum web reinforcement: #4 single bars at 12 in. centers.

In the left-hand-side test, the concentrated load was located at a = 8.5 ft. from the center of bearing. The significant crack exited from the beam at x = 74 in. (the beam top being selected as reference elevation), and intercepted the center line of strands at x = 14 in., providing β = 27.5°.

The crack intercepted five #4 and four #3 bars for a total steel area of 1.423 in^2. At a yield point of 60.0 KSI, the shear - carried by the steel - is 85.4 KIPS, its moment to the B-C line M_s = 2,935 KIP.in. The beam failed at a point load of 168 KIPS; force effects due to this load and the weight of the beam on a 40 ft. span were: V_o = 142.4 KIPS and M_o = 10,764 KIP.in. With a moment arm of 38.65 in., the longitudinal forces $N_c = H_{st}$ = 202.5 KIPS. For a 4,500 PSI concrete - from Table 1 - r = 0.251, providing V_c = 50.8 Kips, or $V_c + V_s$ = 136.2 KIPS. This beam therefore failed in shear.

The bonded length of the strands is 20 in. Using Table 2 - the available resistance H_{st} = 16 x 18.60 = 297.6 KIPS. It is therefore rather unlikely that bond failure had occured.

In the right-hand-side test, the concentrated load was located at a = 10.0 ft. from the center of bearing. The significant crack exited from the beam at x = 120 in. and intercepted the strands at x = 46 in, providing β = 22.9°. The crack intercepted five #4 bars for a steel area of 0.982 in^2. The beam failed at a point load of 245 KIPS on a span of 31.5 ft. providing V_o = 170.6

KIPS and M_o = 20,916 KIP.in. With q = 37.75 in. - N_c =496.8 KIPS. From this V_c = 124.6 KIPS and $V_c + V_s$ = 184.6 KIPS. The ratio between V_o and the shear resistance is 0.924.

The bonded length of strands is 52 in., providing a resistance H_{st} = 16 x 33.56 = 536.9 KIPS. The ratio between required and available strand force is 0.925. The beam therefore had failed at about 7.5% below the theoretical values provided for both shear and slip type failure modes, so this case may be declared to be a boarder line situation.

TWO-SPAN VOIDED SLAB

A quarter size model of a two span continuous, post-tensioned voided slab bridge was tested to failure under a symmetrical loading pattern. As expected the failure was of flexural nature occuring at the internal pier. Calculated force effects were:

M_o = 6,098 KIP.in.

V_o = 77.1 KIPS

M_u = 5,883 KIP.in.

N_c = 705.4 KIPS and

V_c = 151.7 KIPS.

The failure moment exceeded the nominal ultimate moment resistance by 3.6%. The significant crack was entirely vertical, and none of the extensive shear reinforcement had been intercepted. Shear resistance therefore was entirely provided by the concrete due to the large compression force. No shear effect at the failure zone was detected. The calculated shear resistance exceeded the required value by a considerable margin.

8 DISCUSSION OF RESULTS

A total of 34 tests were investigated for this report. Only 25 tests are given in Table 3 since the evidence supporting the validity of the mechanical shear model was found to be largely cumulative.

Failure mode is declared as being flexural if N_c exceeds H_u. There are five such cases listed. For these, both N_c and V_c were adjusted to the nominal H_u value.

There are 13 cases which are declared as shear failures, or rather shear-compression failures in context of the model. According to theory, as presented in Chapter 3, such failure is setting on as the ratio $V_o/(V_c + V_s)$ approaches unity. Statistical evaluation of the 13 tests provides ratios:

average: 0.970

standard deviation: 0.0578, and

95% limit: 0.875.

In other words, the theory seems to over-estimate shear-compression resistance by an average of 3.0%, and the data suggests a resistance factor of 0.875.

There are seven cases which are called as slip failures. In accordance with the mechanical shear model as presented in Chapter 2, such failure is setting on as the ratio N_c/H_{st} approaches unity. Statistical evaluation:

average: 1.151

standard deviation: 0.1478, and

95% limit: 0.908.

The model seems to under-estimate slip resistance by an average of 15.1%. Data suggest a resistance factor of 0.908, but the shear factor of 0.875 - being smaller - governs. Table 3 indicates that the slip failure group is being

dominated by four Purdue tests, all producing very high ratios. Any combination of the following could be responsible for the over-estimate:

a/ crack location was scaled from rough sketches in the test report,

b/ strands surfaces could have been oxidized, providing better bond,

c/ beams had considerable overhangs which appear to have remained intact,

d/ confinement steel being more effective in a relatively small flange.

It is often difficult to determine whether failure is precipitated by shear or by the slip of strands. The model assumes that all active strands slip simultaneously. In reality the slip is gradual - one or two strands at a time - always starting at the top row. As the shear resistance depends to a large degree on the compression force, which in turn is being limited by the anchored strand force, a gradual deterioration by slip may lead to what appears to be a genuine shear failure. It is therefore quite conceivable that the two modes do closely interact. Further errors are also possible due to the subjective discounting of web steel being too close to either end of the crack, due to the actual versus nominal yield point of bars, and due to the actual bond distribution with reference to surface conditions, confinement, mode of release and general cracking.

9 DESIGN ASPECTS

The scope of work for this report does not require turning the shear model into a design methodology. There are, however, three aspects of design which can be formulated conveniently at this time without further investigation.

a/ Flexural Design

As illustrated in Figure 12, the design moment diagram, i.e. the factored extreme moment diagram, may need be adjusted in two ways. First the diagram

is reduced by M_s, the moment of the intercepted web steel force at yield about the B-C line. In order to determine M_s, the arrangement of web steel and location of the significant crack should be known. The reduced diagram is then spread sideways in order to account for the crack intercepting the strands at a location "x" being different from the one external moment was taken at. The need for spreading the design moment diagram has been recognized by other researchers as well; this model only confirms it.

b/ Shear Design

The design, or factored extreme external shear force is resisted by the steel V_s and by the flange concrete V_c. On the other hand $V_c = rM_{os}/q$, where M_{os} is the simultaneous factored external moment. As long as V_o does not exceed rM_{os}/q, only temperature steel is required in the web. This is illustrated in Figure 13 for a 75 ft. simply supported span, in which the inside 52.0 ft. length does not require any consideration for shear.

c/ Continuous Spans

By the same argument as presented above, this model may permit a considerable reduction of web steel adjacent to the internal bearings of continuous spans due to the presence of high bending moments. This case was in a way discussed in conjunction with the voided slab test in Chapter 7.

10 CONCLUSIONS AND RECOMMENDATIONS

The mechanical shear/compression model presented in this report appears to be a reasonably accurate approach to determine the shear resistance of prestressed concrete beams. The mechanical nature of the model is expected to help the designer to visualize the real structural interaction. Shear and moment cannot justifiably separated for the purpose of design, since they tend to interact both ways.

In order to further verify the proposed model, additional tests, carried out by others than the Florida DOT and Purdue University, need be evaluated. Further research is also required to obtain more information on bond distribution with reference to surface condition of the strands, the effect of confinement steel, the effect of the method of release, and the effect of cracking in the anchorage zone. The assumed parabolic distribution of shear stresses in the compression zone also need be verified.

REFERENCES

1/"Shear Design Consideration for Pretensioned Prestressed Beams" by Maruyama and Rizkalla, University of Manitoba.

2/ "Tensile Strength of Concrete" by Cousins and Johnston, University of North Carolina:

3/ "Transfer Lengths in Full Scale AASHTO Prestressed Concrete Beams" by Shahawy, Issa and Batchelor, Florida DOT.

4/ "Analytical and Experimental Evaluation of Stiffness Parameters of Voided Concrete Slab Bridges" by Sen, Issa and Oline, University of South Florida.

5/ "Structural Behavior of High Strength Concrete Prestressed I-Beams" by Kaufman and Ramirez, Purdue University.

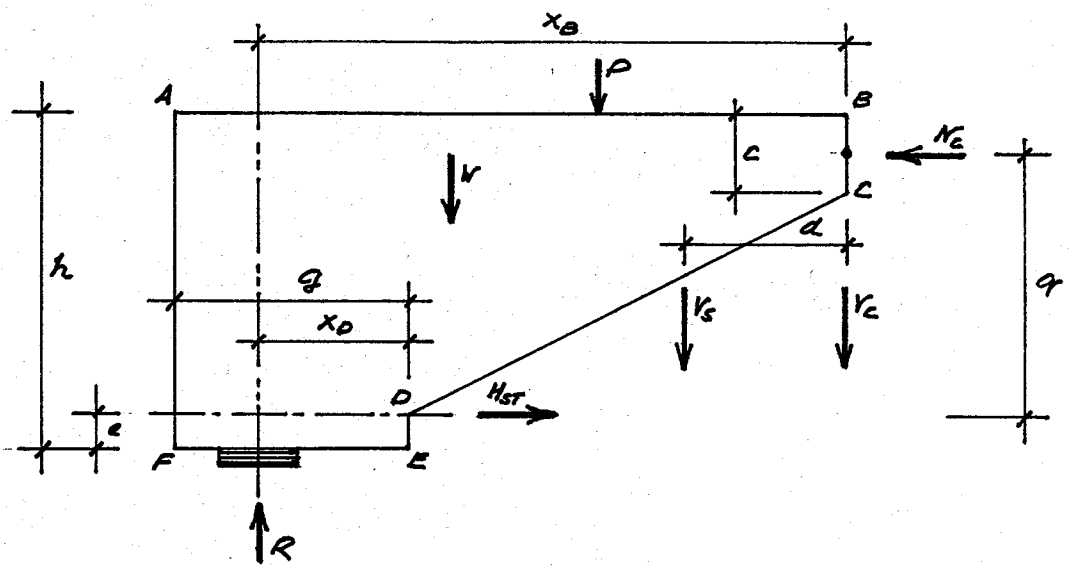

FIGURE 1
THE "CS" SHEAR MODEL

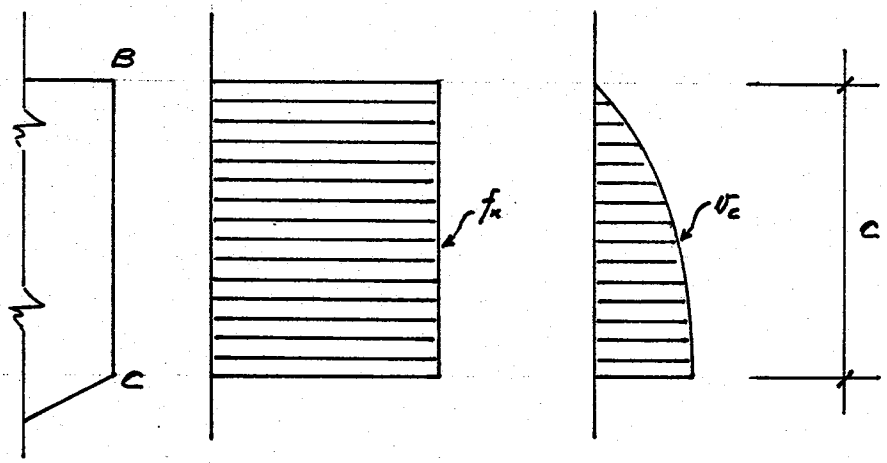

FIGURE 2
ASSUMED STRESS DISTRIBUTIONS IN THE COMPRESSION ZONE

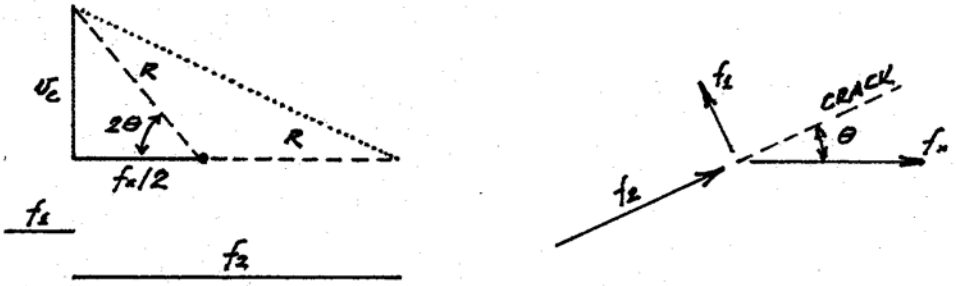

FIGURE 3
PRINCIPAL STRESSES IN THE COMPRESSION ZONE

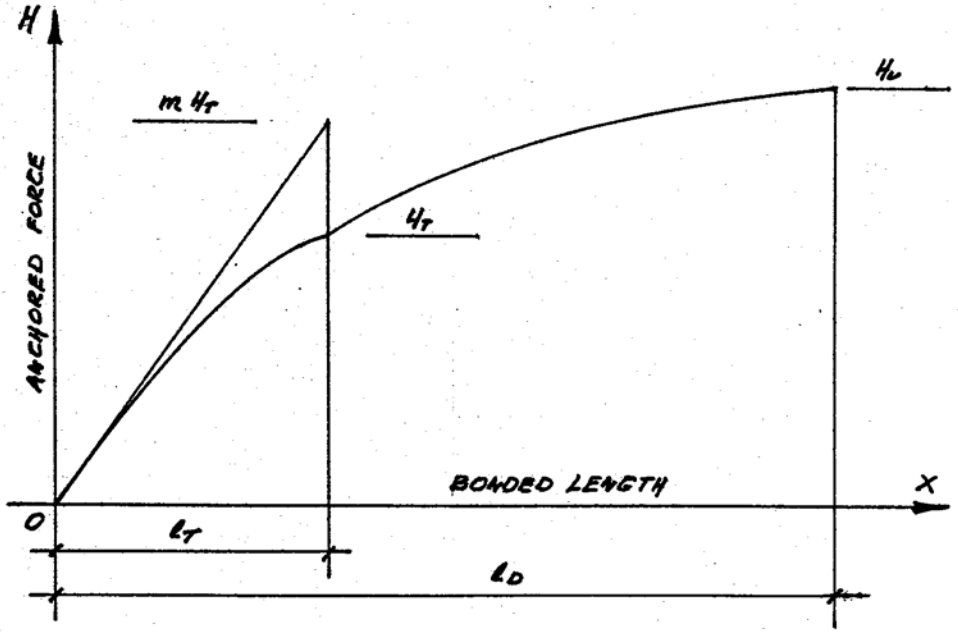

FIGURE 4
DISTRIBUTION OF CUMULATIVE BOND STRESSES

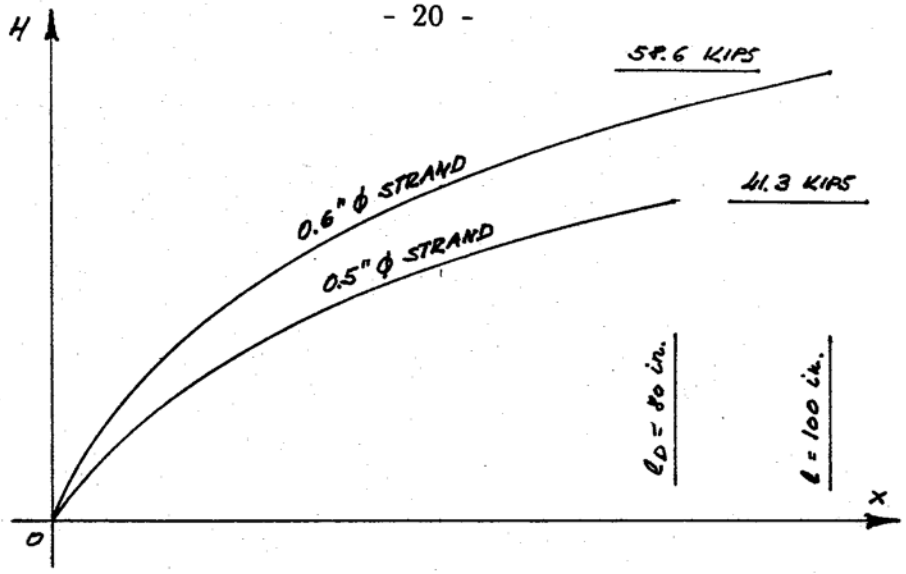

FIGURE 5
IDEALIZED DISTRIBUTION OF CUMULATIVE BOND

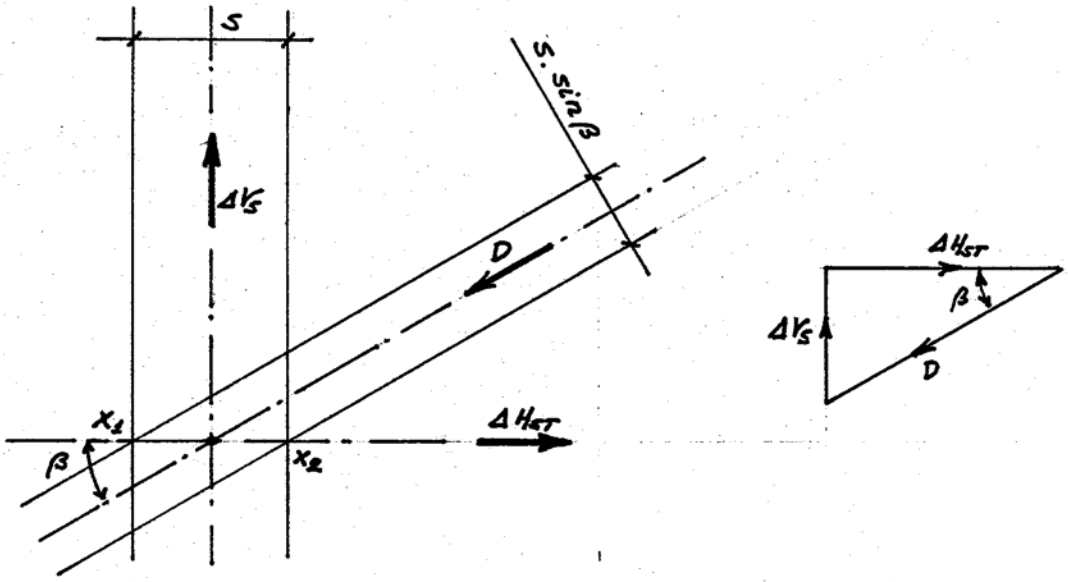

FIGURE 6
STRUT-AND-TIE APPROACH TO WEB FORCES

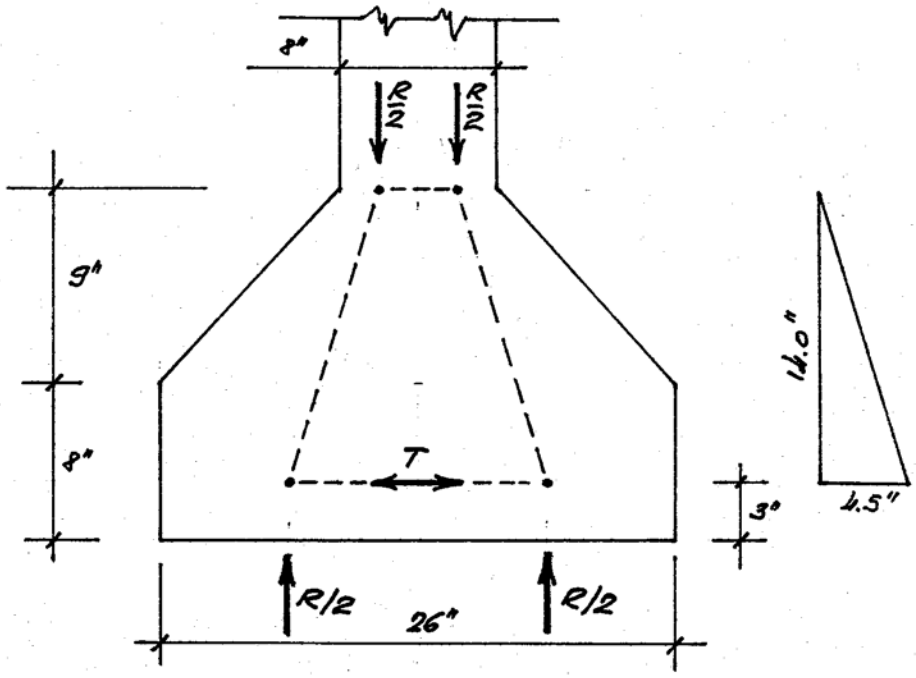

FIGURE 7
SPLITTING FORCE IN BEARING AREA

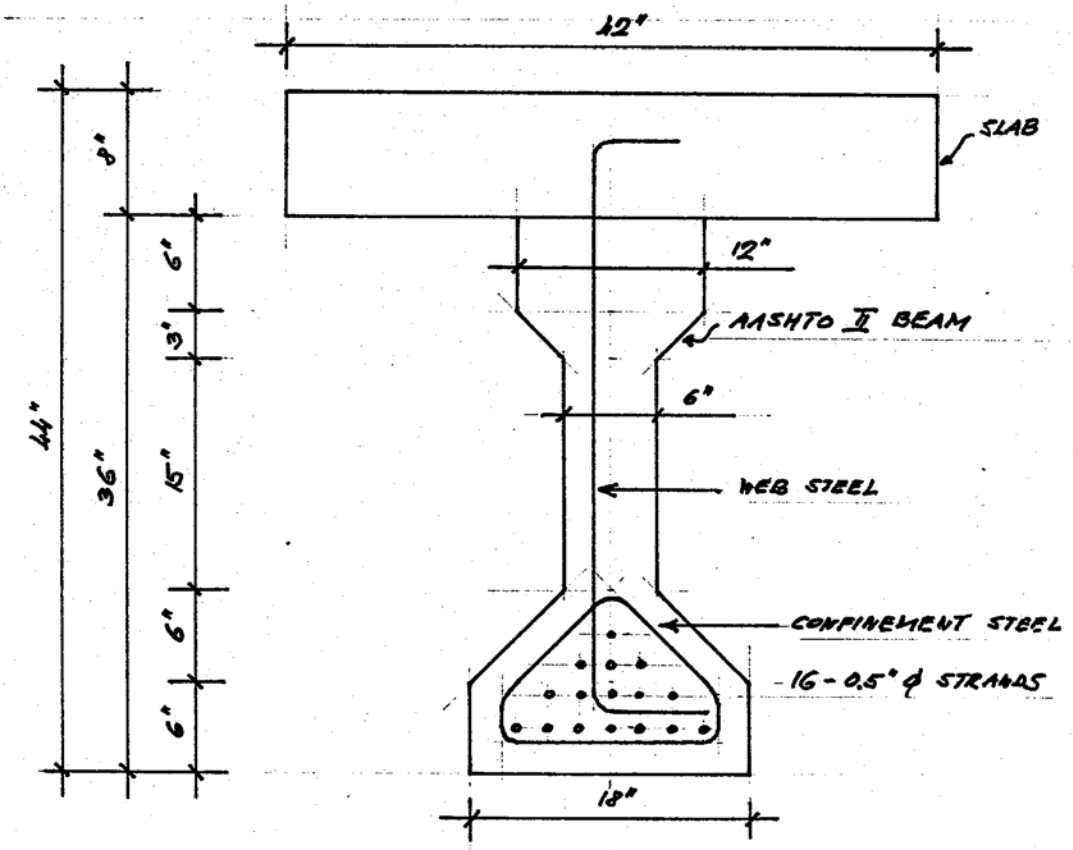

FIGURE 9
CROSS SECTION OF A1-00-M TEST BEAM

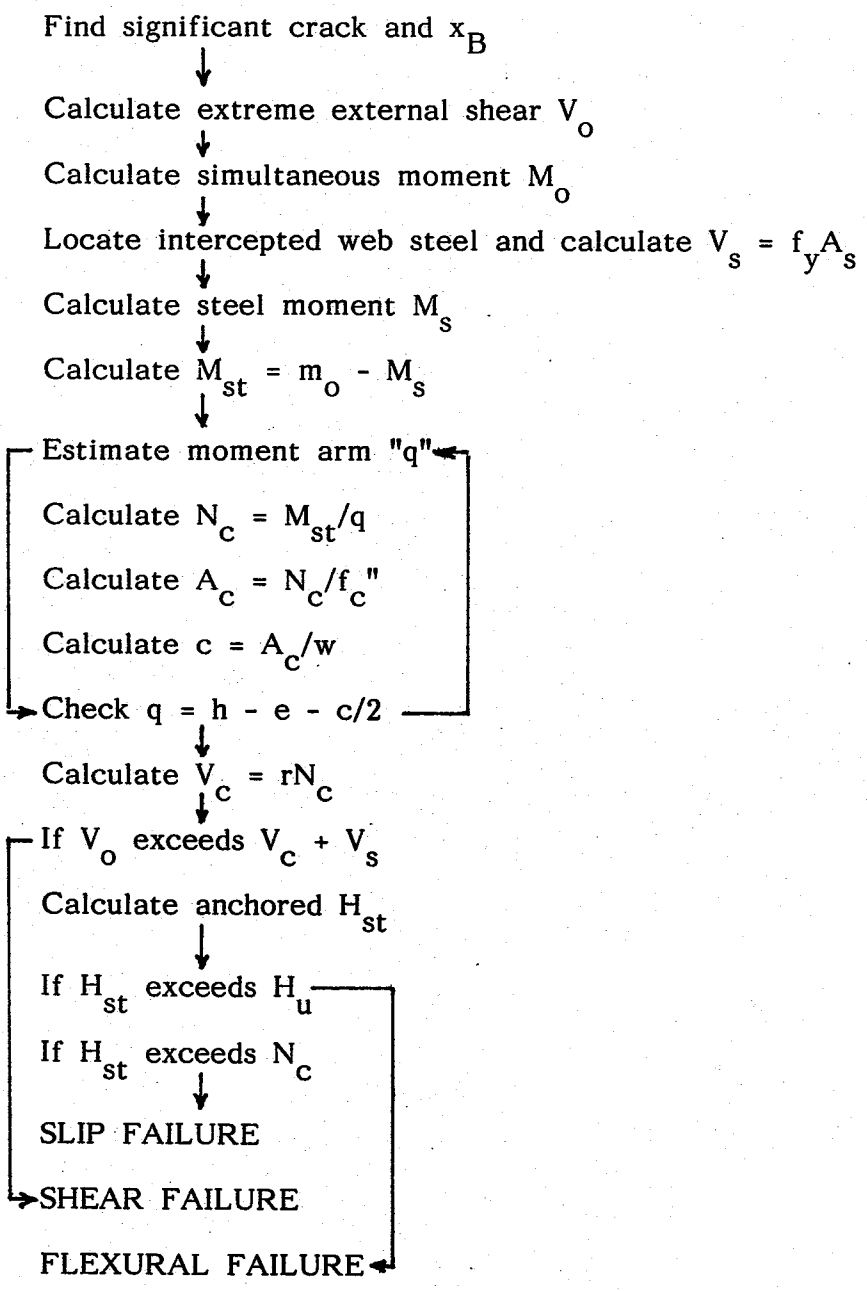

FIGURE 8
FLOW CHART

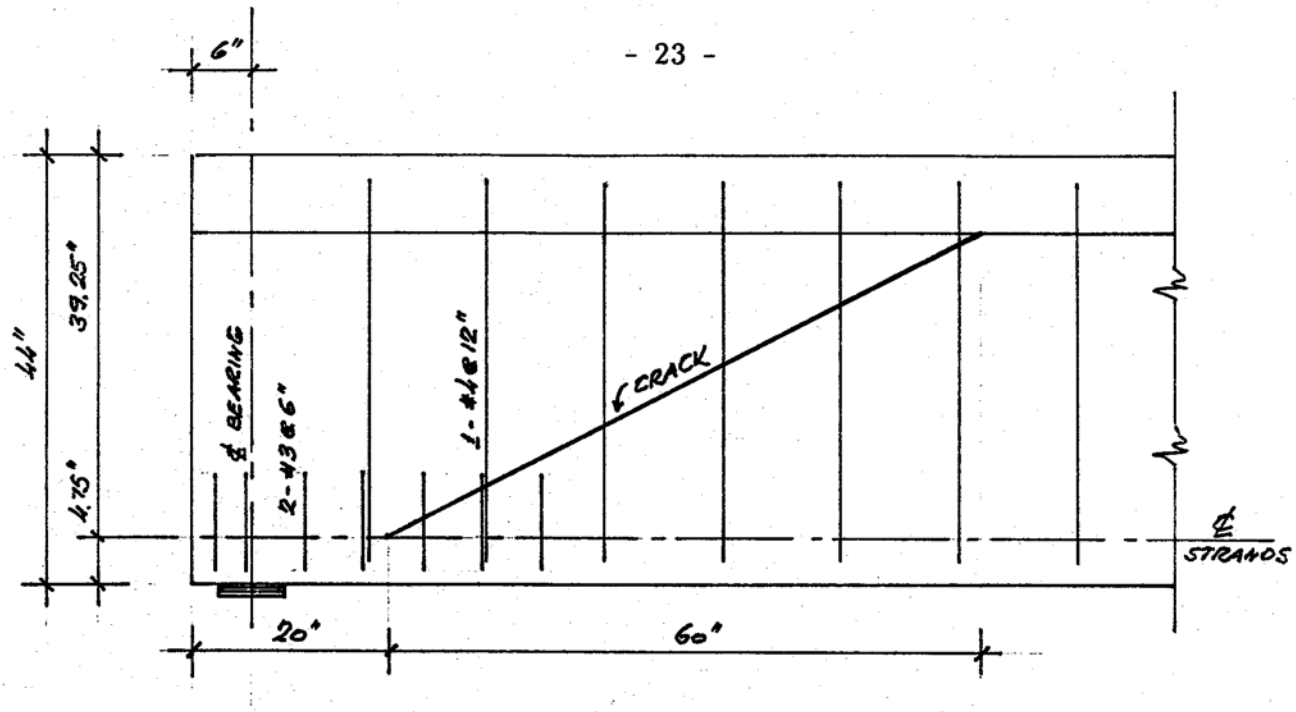

FIGURE 10
CRACK INTERCEPT OF REINFORCEMENT IN TEST A1-00-M-L

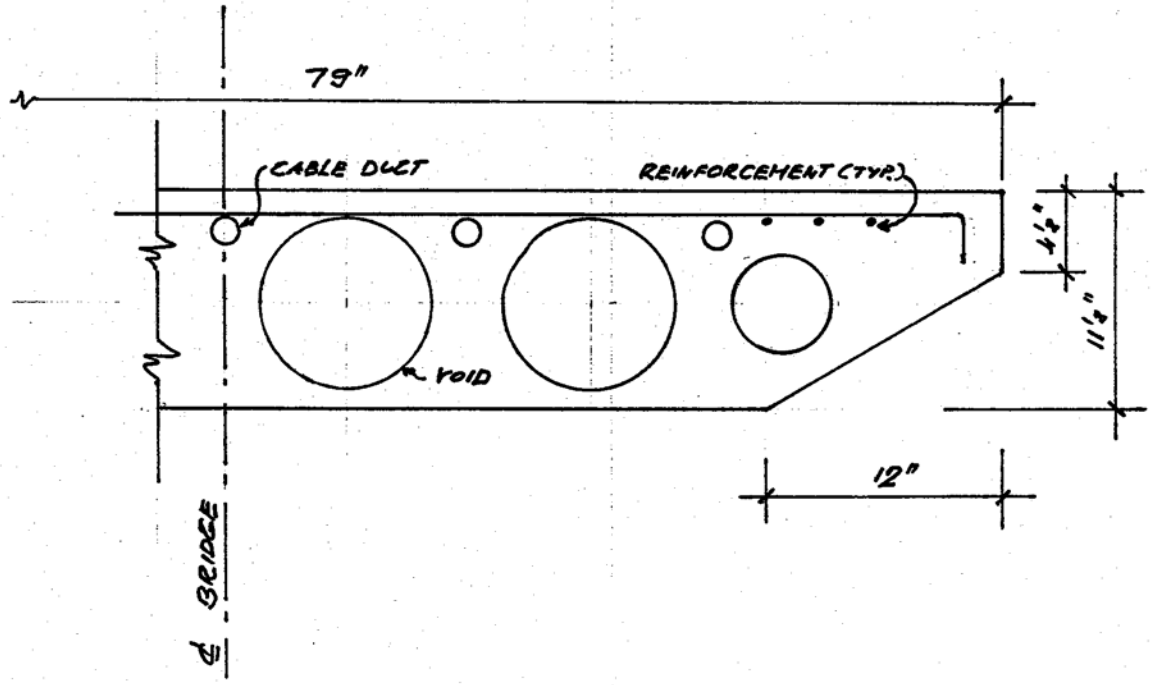

FIGURE 11
CROSS SECTION OF VOIDED SLAB MODEL BRIDGE

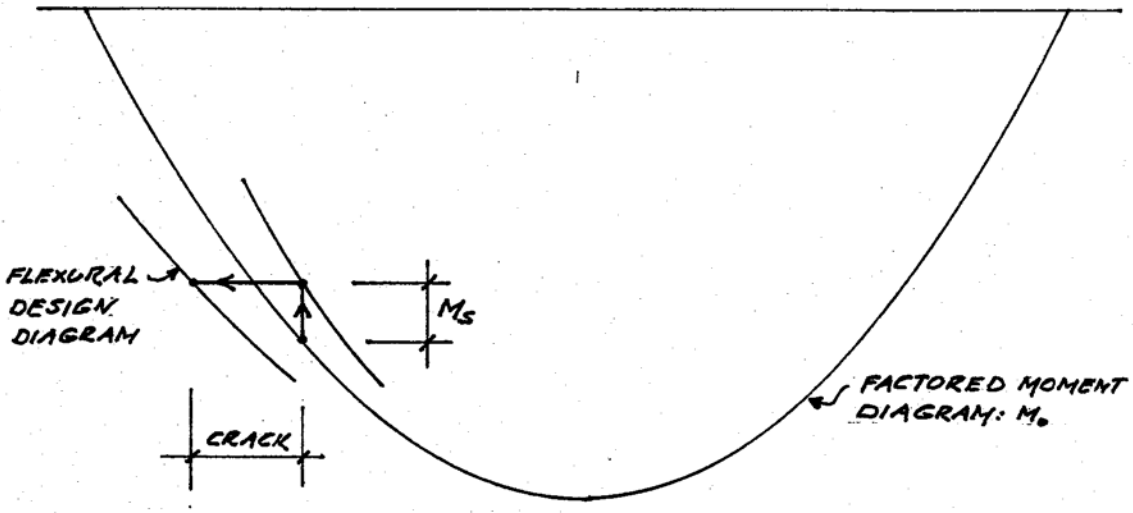

FIGURE 12
PROPOSED FLEXURAL DESIGN

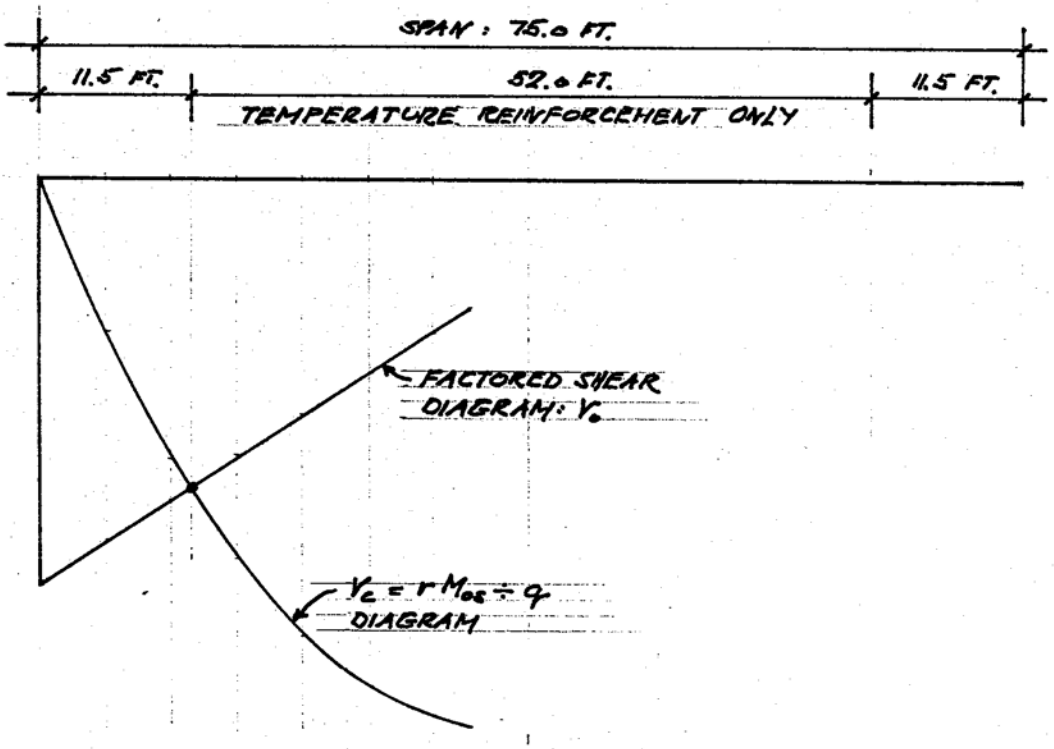

FIGURE 13
PROPOSED SHEAR DESIGN

k		7.5			8.6	
f r I C	k(f f)2 C	f It C	r	k(f r)2 C	f it C	r
2,500	375	2,125	0.304	430 -	2,070	0.334
3,000	411	2,589	0.286	471	2,529	0.313
3,500	444	3,056	0.272	509	2,991	0.298
4,000	474	3,526	0.260	544	3,456	0.285
4,500	503	3,997	0.251	577	3,923	0.274
5,000	530	4,470	0.243	608	4,392	0.265
5,500	556	4,944	0.236	638	4,862	0.257
6,000:	581	5,419	0.230	66	5,334	0.250
6,500	605	5,895:	0.224	693	5,807	0.244
7,000	627	6,373	0.219	20	6,280	0.238
7,500	650	6,850	0.215	745	6,755	0.233
8,000	671	7,329	0.211	769	7,231	0.229
8,500	691	7,809	0.207	793	7,707	0.225
9,000	712	8,288	0.204	816	8,184	0.221
9,500	731	8,769	0.200	838	8,662	0.217
10,000	750	9,250	0.197	860	9,140	0.214

TABLE 1

x	Hx/0.5"D.	H_x/0.6 "D.
05 in.	5.57 KIPS	6.88 KIPS
10	10.50	13.09
15	14.82	18.67
20	18.60	23.63
25	21.89	28.06
30	24.29	31.99
35	27.26	35.44
40	29.44	38.50
45	31.32	41.16
50	32.97	43.51
55	34.45	45.55
60	35.84	47.37
65	37.14	49.02
70	38.46	50.47
75	39.82	51.86
80	41.31	53.14
85		54.42
90		55.75
95	-	57.09
100	-	58.59

TABLE 2

TEST	P t	V o	M o	V s	M s	N c	V c	H st	H V u	/V +V o c s	N /H c st	MODE
A 1-00-M-L	168	142.4	10,764	85.4	2,935	202.5	50.8	297.6	661.0	1.046*	0.680	shear
A 1-00=M-R	245	170.6	20,916	58.9	2,160	496.8	124.6	184.6	661.0	0.924	0.925*	shear/slip
A l-00-R/2=L	200	166:3	16,248	72.0	2,016	373.1	93.6	527.5	661.0	1.004 *	0.707	shear
A l-00-R/2-R	252	174.6	19,920	60.0	1,560 -	485.0	121.6	598.5	661.0	0.961[3]E	0.810	shear
A 1-00-R(D)-L	217	181.5	12,108	144.0	4,277	202.5	50.7	273.4	661.0	0.932 *	0.740	shear
Al-00-R(D)-R	276	190.3	23,508	36.0	,612	61.1.4	153.4	661.0	661.0	1.005*	0.924	shear
A 1-00-R-L	256	210.0	21,744	108.0	2,570	507.9	127.4	590.1'	661.0	0.8923E	0.861	shear
A1-00-R-R	304	207.5	26,184	48.0	,754	661:0	165.8	61.0	661.0)	0.971	1.000	flexure
A 1-00-3 R /2-L	252	206.8	21,408	84.0	1,142	538.3	135.0	661.0	661.0	0.94'	0.814	shear
A 1-00-3 R /2-R	336	229.0	28,848	24.0	,103	661.0	165.8	661.0	661.0	1:206#	1.000	flexure
Voided slab	-	77.1	6,098	-	-	705.4	151.7	-	705.4[3]*E*	0.508	-	flexure
A A S H T O IV-	-	275.5	20,662	199.5	6,585	251.2	65.4	211.5	-	1.040	1.187*	slip
A A S H T O IV-	-	329.0	24,675	199.5	6,585	325.4	84.7	423.0	-	1:117#	0.769	shear
Purdue 1-3	-	101.9	6,144	53.0	1,272	195.3	49.7	141.2	365.0	1.087	1:383*	slip
Purdue II-1	-	141.1	11,736	70.7	2,227	298.6	60.6	236.6	529.1	1.076	1.262*	slip o[n],
Purdue 11-2	-	202.1	17,088	94.2	3,956	420.2'	85.3	360.4	529.1	1.132	1:166*	slip i
Purdue I: 3A	-	113.0	6,804	53.0	1,272	223.1	46:4	190.8	365.0	1.136	1:169*	slip
C 1-00-R-L	220	162.9	23,052	23.6	,330	598.7	150.2	644.5	644.5	0.937*	0.929	shear
C 1-00-R-R	220	145.9	19,788	23.6	,000	518.0	129.9	644.5	644.5	0.950#	0.804	shear
C l-00-R(D)-L	231	164.8	25,248	23.6	,212	644.5	161.7	644.5	644.5[3]	0.889	1.000	flexure
C l-00-R(D)-R	252	154.2	23,664	11.8	,059	623.6	156.4	644.5	644.5	0.917	0.967[3]E	slip
C1-00-3R/2-L	237	160.8	21,756	35.4	,354	562.5	141.4	644.5	644.5	0.911'	0.873	shear
C 1-00-3 R /2-R	227	154.4	19,572	35.4	,354	503.1	126.2	644.5	644.5	0.955#	0.781	shear
C l-25-R	-	155.4	22,356	58.9	1,178	483.4	121.2	483.4	483.4[3]	0.863	1.151	flexure
D-00-R C	232	212.8	13,320	164.9	4,288	231.6	58.1	270.2	644.5	0.954iE	0.857	shear

NOTES: P_t single ultimate test load where applicable

All forces in KIPS, all moments in KIP.in:

Purdue University tests from Reference 5.

TABLE 3